Meccanica (2013) 48:1415–1430
DOI 10.1007/s11012-012-9675-6

Impact of thermophoresis particle deposition and chemical reaction on unsteady non-Darcy mixed convective flow over a porous wedge in the presence of temperature-dependent viscosity

I. Muhaimin · R. Kandasamy · Azme B. Khamis · Rozani bin Roslan

Received: 10 April 2012 / Accepted: 26 November 2012 / Published online: 11 December 2012

Abstract An analysis is presented to investigate the effect of thermophoresis particle deposition and temperature dependent viscosity on unsteady non-Darcy mixed convective heat and mass transfer of a viscous and incompressible fluid past a porous wedge in the presence of chemical reaction. The wall of the wedge is embedded in a uniform non-Darcian porous medium in order to allow for possible fluid wall suction or injection. The governing partial differential equations of the problem, subjected to their boundary conditions, are solved numerically by applying an efficient solution scheme for local nonsimilarity boundary layer analysis. Numerical calculations are carried out for different values of dimensionless parameters arising in the problem. The results are compared with available ones in the literature and excellent agreement is obtained. An analysis of the obtained results shows that the flow field is influenced appreciably by the chemical reaction and thermophoresis particle deposition.

Keywords Unsteady flow · Temperature dependent viscosity · Thermophoresis · Chemical reaction and non-Darcy flow

I. Muhaimin · R. Kandasamy (✉) · A.B. Khamis · R. bin Roslan
Research Centre for Computational Mathematics, FSTPi, Universiti Tun Hussein Onn Malaysia, Batu Pahat, Johor, Malaysia
e-mail: future990@gmail.com

Nomenclature

C	Species concentration in the boundary layer [kg m^{-2}]
c_p	Specific heat due to constant pressure [J kg^{-1} K^{-1}]
C_w	Species concentrations of wall
C_∞	Species concentrations of the ambient fluid
D	Molecular diffusivity
f	Dimensionless stream function
N_t	Thermophoresis parameter
Pr_A	Ambient Prandtl number
Pr_v	Variable Prandtl number
Re_x	Local Reynolds number
Sc	Schmidt number
T	Temperature of the fluid
T_w	Temperature at the wall surface
T_r	Reference temperature of the fluid [K]
T_∞	Temperature of the ambient fluid [K]
x, y	Axis in direction along and normal to the wedge [m]
U	Free stream velocity [m s^{-1}]
u, v	The x- and y-component of the velocity field [m s^{-1}]
V_T	Thermophoretic velocity

Greek symbols

β_1	Wedge angle parameter
γ	Chemical reaction parameter
δ	Time dependent length scale
κ	Thermophoretic coefficient defined
ρ	Fluid density [kg m^{-3}]

ψ Stream function [$m^2\,s^{-1}$]
η Similarity variable
ν Kinematic viscosity [$m^2\,s^{-1}$]
μ Fluid viscosity [Pa s]
μ_∞ Ambient fluid viscosity [Pa s]
τ Thermophoretic parameter
θ Dimensionless temperature
ϕ Dimensionless concentration
λ_u Unsteadiness parameter

1 Introduction

Thermophoresis, described as a physical phenomenon in which aerosol particles, subjected to a temperature gradient, move from high- to low-temperature zones of the gas, has attracted considerable attention for collection of submicrometer and nanometer particles. Viscous heating plays an important role in the dynamics of fluids with strongly temperature-dependent viscosities because of the coupling between the energy and momentum equations. Impurity ions may move from the cold side of a semiconductor wafer towards the hot side, since the higher temperature makes the transition structure required for atomic jumps more achievable. The diffusive flux may occur in either direction (either up or down the temperature gradient), dependent on the materials involved. Thermophoretic force has been used in commercial precipitators for applications similar to electrostatic precipitators. It is exploited in the manufacturing of optical fiber in vapor deposition processes. It can be important as a transport mechanism in fouling. Thermophoresis has also been shown to have potential in facilitating drug discovery by allowing the detection of aptamer binding by comparison of the bound versus unbound motion of the target molecule. This approach has been termed microscale thermophoresis. Thermophoresis is one of the methods used to separate different polymer particles in field flow fractionation. In particular, the contaminant particle deposition onto the surface of products in the electronic industry plays a critical role in the resulting product quality.

Thermophoresis with temperature dependent viscosity is an important mechanism of micro-particle transport due to a temperature gradient in the surrounding medium and has found numerous applications, especially in the field of aerosol technology. When the temperature gradient exists in the fluid surrounding a small particle, a net force is exerted on the particle due to an imbalance of the forces associated with molecular collisions from the hotter and colder regions. In most cases the force is in the direction of the cold region. In certain porous media applications such as those involving heat removal from nuclear fuel debris, underground disposal of radioactive waste material, storage of food stuffs, and exothermic and/or endothermic chemical reactions and dissociating fluids in packed-bed reactors, the working fluid thermophoresis particle deposition effects are important. In the application of pigments, or chemical coating of metals, or removal of particles from a gas stream by filtration, there can be distinct advantages in exploiting deposition mechanisms to improve efficiency. Thermophoretic deposition of radioactive particles is considered to be one of the important factors causing accidents in nuclear reactors. Acid rain is caused by emissions of sulfur dioxide and nitrogen oxides, which react with the water molecules in the atmosphere to produce acids. China government has made efforts since the 1970s to reduce the release of sulfur dioxide into the atmosphere with positive results. Nitrogen oxides can also be produced naturally by lightning strikes and sulfur dioxide is produced by volcanic eruptions. The chemicals in acid rain can cause paint to peel, corrosion of steel structures such as bridges, and erosion of stone statues. Thermophoresis particle deposition with chemical reaction in the presence of magnetic field plays an important role on the rapid growth of World's economy and has led to severe air pollution characterized by acid rain, severe pollution in cities, and regional air pollution. High concentrations are found for various pollutants such as sulfur dioxides (SO_2), nitrogen oxides (NO_x), and fine particulates. Great efforts have thus been undertaken for the control of air pollution in the country.

The effects of thermophoresis particle deposition with temperature dependent viscosity on forced and free convection flows are also important in the context of space technology and processes involving high temperatures. In light of these various applications, Tsai and Lin [1] proposed an approach through numerical integration for evaluating the particle deposition rates. Selim et al. [2] investigated the effect of surface mass transfer on mixed convection flow past a heated vertical flat permeable plate with thermophore-

sis. Seddeek [3] studied the influence of viscous dissipation and thermophoresis on Darcy–Forchheimer mixed convection in a fluid saturated porous media. Postelnicu [4] studied the effects of thermophoresis particle deposition in free convection boundary layer from a horizontal flat plate embedded in a porous medium. Alam et al. [5], [6] and [7] analyzed the effects of thermophoresis on steady two-dimensional hydromagnetic heat, and mass transfer flow over an inclined flat plate with various flow conditions. Goldsmith and May [8] first studied the thermophoretic transport involved in a simple one-dimensional flow for the measurement of the thermophoretic velocity. Thermophoresis in laminar flow over a horizontal flat plate has been studied theoretically by Goren [9]. Thermophoresis in natural convection with variable properties for a laminar flow over a cold vertical flat plate has been studied by Jayaraj et al. [10]. The first analysis of thermophoretic deposition in geometry of engineering interest appears to be that of Hales et al. [11]. They have solved the laminar boundary layer equations for simultaneous aerosol and steam transport to an isothermal vertical surface situated adjacent to a large body of an otherwise quiescent air-steam-aerosol mixture. Chamkha et al. [12] studied the effect of thermophoresis of aerosol particles in the laminar boundary layer on a flat plate. Chamkha and Pop [13] studied the effect of thermophoresis particle deposition in free convection boundary layer from a vertical flat plate embedded in a porous medium. Duwairi and Damseh [14] analyzed the effect of thermophoresis particle deposition on mixed convection from vertical surfaces embedded in saturated porous medium with variable wall temperature and concentration. Recently, Rahman and Postelnicu [15] performed the effects of thermophoresis on the forced convective laminar flow of a viscous incompressible fluid over a rotating disk.

Effects of heat and mass transfer on mixed convection flow in the presence of suction/injection have been studied by many authors in different situations. But so far no attempt has been made to analyze the effects of thermophoresis particle deposition with chemical reaction on unsteady non-Darcy mixed convective heat and mass transfer past a porous wedge in the presence of temperature-dependent viscosity and hence we have considered the problem of this kind. One of the main focuses behind this study is also to investigate how the magnetic strength and

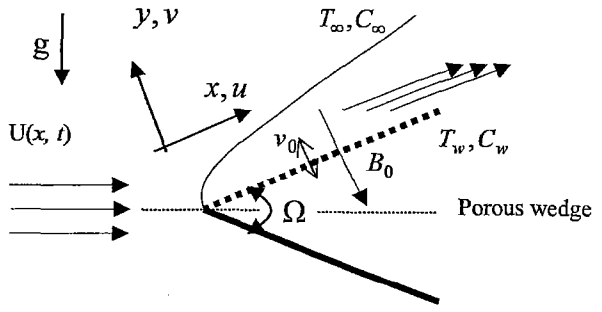

Fig. 1 Flow analysis along the wall of the wedge

thermophoresis particle deposition varies within the boundary layer when the viscosity is dependent on temperature. By introducing a new class of similarity transformation proposed by Sattar [16], the governing non-linear partial differential equation is reduced to locally similar ordinary differential equation, which was solved numerically by applying shooting method and the results were discussed from the physical point of view. It is hoped that the results obtained will not only provide useful information for applications, but also serve as a complement to the previous studies.

2 Formulation of the problem

Let us consider an unsteady, laminar, hydromagnetic coupled heat and mass transfer by mixed convection flow in front of a stagnation point on a wedge plate embedded in porous medium. The fluid is assumed to be Newtonian and its property variations due to temperature are limited to density and viscosity. The density variation and the effects of the buoyancy are taken into account in the momentum equation (Boussinesq's approximation) and the concentration of species far from the wall, C_∞, is infinitesimally small. Let the x-axis be taken along the direction of the wedge and y-axis normal to it. The chemical reaction is taking place in the flow and the effect of thermophoresis is being taken into account to help in the understanding of the mass deposition variation on the surface. Fluid suction or injection is imposed at the wedge surface, see Fig. 1. Under these conditions, the governing boundary layer equations of momentum, energy and diffusion for mixed convection flow neglecting Joule's viscous dissipation under Boussinesq's approximation including variable viscosity are

$$\frac{\partial u}{\partial x}+\frac{\partial v}{\partial y}=0 \tag{1}$$

$$\begin{aligned}\frac{\partial u}{\partial t}+u\frac{\partial u}{\partial x}+v\frac{\partial u}{\partial y}&=\frac{\partial U}{\partial t}+\frac{1}{\rho}\frac{\partial}{\partial y}\left(\mu\frac{\partial u}{\partial y}\right)+U\frac{dU}{dx}\\&\quad-\frac{F}{\sqrt{K}}\left(u^2-U^2\right)-\frac{\nu}{K}(u-U)\\&\quad+\left\{g\beta(T-T_\infty)+g\beta^*(C-C_\infty)\right\}\sin\frac{\Omega}{2}\end{aligned} \tag{2}$$

$$\frac{\partial T}{\partial t}+\rho c_p\left(u\frac{\partial T}{\partial x}+v\frac{\partial T}{\partial y}\right)=k_e\frac{\partial^2 T}{\partial y^2}+\mu\left(\frac{\partial u}{\partial y}\right)^2 \tag{3}$$

$$\frac{\partial C}{\partial t}+u\frac{\partial C}{\partial x}+v\frac{\partial C}{\partial y}=D\frac{\partial^2 C}{\partial y^2}-\frac{\partial(V_T C)}{\partial y}-k_1 C. \tag{4}$$

The boundary conditions are,

$$u=0,\qquad v=-v_0,\qquad T=T_w,\qquad C=C_w \quad \text{at } y=0 \tag{5}$$

$$u=U(x,t),\qquad T=T_\infty,\qquad C=C_\infty \quad \text{at } y\to\infty \tag{6}$$

where u, v are the velocity components in the x and y directions respectively, t is the time, D is the effective diffusion coefficient; μ is the dynamic viscosity, ρ is the fluid ambient density, c_p is the specific heat at constant pressure and k_e is the porous medium effective thermal conductivity, ν is the kinematic viscosity of the fluid, k_1 (is the rate of chemical reaction in Eq. (4)) can be adjusted to meet these circumstances if one takes (i) $k_1>0$ for destructive reaction, (ii) $k_1=0$ for no reaction and (iii) $k_1<0$ for generative reaction, K is the permeability of the porous medium, V_T $(=-k\frac{\nu}{T}\frac{\partial T}{\partial y})$ is the thermophoretic velocity, where k is the thermophoretic coefficient (see Talbot et al. [17]) and F is the empirical constant in the second order resistance and setting $F=0$ in Eq. (2) is reduced to the Darcy law. The fourth and fifth terms on the right-hand side of Eq. (2) stand for the first-order (Darcy) resistance and second-order (porous inertia) resistance, respectively. The first step was to predict the pressure and velocity within the porous medium.

The fluid properties are assumed to be constant, except for the fluid viscosity μ which is assumed to vary as an inverse linear function of temperature, in the form (Pantokratoras [18]);

$$\frac{1}{\mu}=\frac{1}{\mu_\infty}\left[1+\gamma_t(T-T_\infty)\right] \quad\text{and}\quad \frac{1}{\mu}=d(T-T_\infty) \tag{7}$$

where $d=\frac{\gamma_t}{\mu_\infty}$ and $T_r=T_\infty-\frac{1}{\gamma_t}$.

Both d and T_∞ are constant and their values depend on the reference state and the thermal property of the fluid, i.e. γ_t. In general, $d>0$ for liquids and $d<0$ for gases. Consider the uniform flow of velocity U_∞ and temperature T_∞ through a highly porous medium bounded by a wall of the wedge parallel to the flow. Also, θ_r is a constant which is defined by

$$\theta_r=\frac{T_r-T_\infty}{T_w-T_\infty}=\frac{1}{\gamma_t(T_w-T_\infty)}. \tag{8}$$

It is worth mentioning here that for $\gamma_t\to 0$ i.e. $\mu=\mu_\infty$ (constant) then $\theta_r\to\infty$. It is also important to note that θ_r is negative for liquids and positive for gases. The flow model is based on the following assumption that the flow is unsteady, incompressible, laminar and the fluid viscosity which is assumed to be an inverse linear function of temperature.

Following the lines of Kafoussias and Nanousis [19], the following change of variables are introduced

$$\begin{aligned}\eta&=y\sqrt{\frac{(1+m)}{2}}\sqrt{\frac{x^{m-1}}{\delta^{m+1}}},\\ \psi&=\sqrt{\frac{2}{1+m}}\frac{\nu x^{\frac{m+1}{2}}}{\delta^{\frac{m+1}{2}}}f(\eta),\\ \theta&=\frac{T-T_\infty}{T_w-T_\infty}\quad\text{and}\quad\phi=\frac{C-C_\infty}{C_w-C_\infty}.\end{aligned} \tag{9}$$

Under this consideration, the potential flow velocity of the wedge can be written as

$$U(x,t)=\frac{\nu x^m}{\delta^{m+1}},\qquad \beta_1=\frac{2m}{1+m} \quad \text{(see in Sattar [16])} \tag{10}$$

where m is an arbitrary constant and related to the wedge angle and β_1 is the Hartree pressure gradient parameter that corresponds to $\beta_1=\frac{\Omega}{\pi}$ for a total angle Ω of the wedge whereas δ is the time-dependent length scale which is taken to be (detailed in Sattar [20]) as $\delta=\delta(t)$.

The continuity equation (1) is satisfied by the stream function $\psi(x,y)$ and it is defined as

$$u=\frac{\partial\psi}{\partial y}\quad\text{and}\quad v=-\frac{\partial\psi}{\partial x} \tag{11}$$

Equations (2) to (4) become

$$(\theta-\theta_r)\frac{\partial^3 f}{\partial\eta^3}=\frac{(\theta-\theta_r)^2}{\theta_r}\left\{-f\frac{\partial^2 f}{\partial\eta^2}-\frac{2m}{1+m}\left(1-\left(\frac{\partial f}{\partial\eta}\right)^2\right)-\frac{2}{1+m}\gamma_1(\theta+N\phi)\sin\frac{\Omega}{2}\right.$$
$$+\frac{2x}{1+m}\left(\frac{\partial f}{\partial\eta}\frac{\partial^2 f}{\partial x\partial\eta}-\frac{\partial f}{\partial x}\frac{\partial^2 f}{\partial\eta^2}\right)+\frac{2}{m+1}\frac{\nu x}{KU}\left(\frac{\partial f}{\partial\eta}-1\right)+\frac{2}{m+1}\left(\frac{Fx}{\sqrt{K}}\right)\left(\left(\frac{\partial f}{\partial\eta}\right)^2-1\right)$$
$$\left.+\frac{\delta^m}{\nu x^{m-1}}\frac{\partial\delta}{\partial t}\left(2-2\frac{\partial f}{\partial\eta}-\eta\frac{\partial^2 f}{\partial\eta^2}\right)\right\}+\frac{2}{m+1}\frac{\partial\theta}{\partial\eta}\frac{\partial^2 f}{\partial\eta^2} \tag{12}$$

$$\frac{\partial^2\theta}{\partial\eta^2}=-\mathrm{Pr}_A\frac{\partial\theta}{\partial\eta}+\frac{2\mathrm{Pr}_A}{1+m}\theta\frac{\partial f}{\partial\eta}+\mathrm{Pr}_A\frac{2x}{1+m}\left(\frac{\partial f}{\partial\eta}\frac{\partial\theta}{\partial x}-\frac{\partial f}{\partial x}\frac{\partial\theta}{\partial\eta}\right)-\mathrm{Pr}_A Ec\left(\frac{\partial^2 f}{\partial\eta^2}\right)^2-\mathrm{Pr}_A\frac{\delta^m}{\nu x^{m-1}}\frac{\partial\delta}{\partial t}\eta\frac{\partial\theta}{\partial\eta} \tag{13}$$

$$\frac{\partial^2\phi}{\partial\eta^2}=-Sc\left(f-\tau\frac{\partial\theta}{\partial\eta}\right)\frac{\partial\phi}{\partial\eta}+\frac{2Sc}{1+m}\phi\frac{\partial f}{\partial\eta}+\frac{2xSc}{1+m}\left(\frac{\partial f}{\partial\eta}\frac{\partial\phi}{\partial x}-\frac{\partial f}{\partial x}\frac{\partial\phi}{\partial\eta}\right)-\mathrm{Pr}\frac{\delta^m}{\nu x^{m-1}}\frac{\partial\delta}{\partial t}\eta\frac{\partial\phi}{\partial\eta}$$
$$+Sc\,\tau\frac{\partial^2\theta}{\partial\eta^2}\phi+\frac{2Scx}{1+m}\phi\gamma. \tag{14}$$

In order to make Eqs. (12) to (14) locally similar, let $\lambda_u=\frac{\delta^m}{\nu x^{m-1}}\frac{\partial\delta}{\partial t}$, where λ_u is taken to be a constant and it can be treated as a dimensionless measure of the unsteadiness.

The Grashof number Gr_x, Local buoyancy parameter γ_1, Sustentation parameter N, Reynolds number Re_x, Modified local Reynolds number Re_k, Ambient Prandtl number Pr_A, Forchheimer number F_n, chemical reaction parameter γ, Schmidt number Sc, magnetic parameter M^2, thermophoresis particle deposition parameter τ, Eckert number, E_c and porous medium parameter λ, are defined as

$$Gr_x=\frac{g\beta(T_w-T_\infty)\delta^{3m+3}}{\nu^2x^{3m}},\qquad \gamma_1=\frac{Grx}{\mathrm{Re}\,x},\qquad \mathrm{Re}_x=\frac{x^{m+1}}{\delta^{m+1}},\qquad \mathrm{Re}_k=\frac{x^m\sqrt{K}}{\delta^{m+1}},\qquad \mathrm{Pr}_A=\frac{\nu}{\alpha_e}$$

(where α_e is the effective thermal diffusivity of the porous medium)

$$\alpha_e=\left(\frac{k_e}{\rho c_p}\right),\qquad F_n=\frac{x^mF\sqrt{K}}{\delta^{m+1}},\qquad \gamma=\frac{\delta^{2m+2}k_1}{\nu x^{2m}},\qquad Sc=\frac{\nu}{D},\qquad \tau=-\frac{k(T_w-T_\infty)}{T_r}, \tag{15}$$
$$E_c=\frac{c^2}{c_p(T_w-T_\infty)}\left(k^2\right)^{\frac{2m}{1-m}}\quad\text{and}\quad \lambda=\frac{\delta^{m+1}}{Kx^{m-1}}$$

The value of θ_r is determined by the viscosity of the fluid under consideration and the operating temperature deference. If θ_r is large, in other words, if $T_\infty - T_w$ is small, the effects of variable viscosity can then be neglected. On the other hand, for a smaller value of θ_r either the fluid viscosity changes significantly with temperature or the operating temperature is high. In either case, the variable viscosity effect is expected to become very important.

The boundary conditions can be written as

$$\eta=0:\quad \frac{\partial f}{\partial\eta}=0,$$
$$\frac{f}{2}\left(1+\frac{x}{U}\frac{dU}{dx}\right)+x\frac{\partial f}{\partial x}=-v_0\sqrt{\frac{(1+m)x}{2\nu U}}, \tag{16}$$
$$\theta=1,\ \phi=1$$
$$\eta\to\infty:\quad \frac{\partial f}{\partial\eta}=1,\quad \theta=0,\ \phi=0$$

where v_0 is the velocity of suction if $v_0<0$ and injection if $v_0>0$.

Equations (12) to (14) and boundary conditions (16) can be written as

$$\frac{\partial^3 f}{\partial \eta^3}+\frac{(\theta-\theta_r)}{\theta_r}\left\{\left(f\frac{\partial^2 f}{\partial \eta^2}+\frac{1-m}{1+m}\xi\left(\frac{\partial f}{\partial \xi}\frac{\partial^2 f}{\partial \eta^2}-\frac{\partial^2 f}{\partial \xi\,\partial \eta}\frac{\partial f}{\partial \eta}\right)+\frac{2}{1+m}\gamma_1(\theta+N\phi)\sin\frac{\Omega}{2}-\frac{2}{m+1}\xi^2\lambda\left(\frac{\partial f}{\partial \eta}-1\right)\right.\right.$$
$$\left.\left.-\frac{2}{m+1}\left(\left(\frac{\partial f}{\partial \eta}\right)^2-1\right)\left(\frac{\mathrm{Re}\,x}{\mathrm{Re}_k}F_n+m\right)\right)-\frac{\delta^m}{\nu x^{m-1}}\frac{\partial \delta}{\partial t}\left(2-2\frac{\partial f}{\partial \eta}-\eta\frac{\partial^2 f}{\partial \eta^2}\right)\right\}$$
$$-\frac{2}{1+m}\left(\frac{1}{\theta-\theta_r}\right)\frac{\partial \theta}{\partial \eta}\frac{\partial^2 f}{\partial \eta^2}=0 \tag{17}$$

$$\frac{\partial^2 \theta}{\partial \eta^2}+\mathrm{Pr}_A\left(f\frac{\partial \theta}{\partial \eta}+\frac{1-m}{1+m}\xi\left(\frac{\partial f}{\partial \xi}\frac{\partial \theta}{\partial \eta}-\frac{\partial \theta}{\partial \xi}\frac{\partial f}{\partial \eta}\right)\right)-\frac{2\mathrm{Pr}_A}{1+m}\theta\frac{\partial f}{\partial \eta}+\mathrm{Pr}_A\,E_c\left(\frac{\partial^2 f}{\partial \eta^2}\right)^2+\mathrm{Pr}_A\frac{\delta^m}{\nu x^{m-1}}\frac{\partial \delta}{\partial t}\eta\frac{\partial \theta}{\partial \eta}=0 \tag{18}$$

$$\frac{\partial^2 \phi}{\partial \eta^2}+Sc\left(f-\tau\frac{\partial \theta}{\partial \eta}\right)\frac{\partial \phi}{\partial \eta}+Sc\frac{1+m}{1-m}\left(\frac{\partial \phi}{\partial \eta}\xi\frac{\partial f}{\partial \xi}-\frac{\partial f}{\partial \eta}\xi\frac{\partial \phi}{\partial \xi}\right)-\frac{2Sc}{1+m}\phi\frac{\partial f}{\partial \eta}-\frac{2Sc}{1+m}\xi^2\gamma\phi$$
$$+Sc\frac{\delta^m}{\nu x^{m-1}}\frac{\partial \delta}{\partial t}\eta\frac{\partial \phi}{\partial \eta}-Sc\tau\frac{\partial^2 \theta}{\partial \eta^2}\phi=0 \tag{19}$$

$$\eta=0:\quad \frac{\partial f(\xi,\eta)}{\partial \eta}=0,\qquad \frac{(1+m)}{2}f(\xi,\eta)+\frac{1-m}{2}\xi\frac{\partial f(\xi,\eta)}{\partial \xi}=-S,\qquad \theta(\xi,\eta)=1,\qquad \phi(\xi,\eta)=1$$
$$\eta\to\infty:\quad \frac{\partial f(\xi,\eta)}{\partial \eta}=1,\qquad \theta(\xi,\eta)=0,\qquad \phi(\xi,\eta)=0 \tag{20}$$

where $S=\frac{v_0}{\nu}\sqrt{\frac{(m-1)\delta^{m+1}}{2x^{m-1}}}$ is the suction parameter if $S>0$ and injection if $S<0$, F_n is the dimensionless inertial parameter (Forchheimer number) and $\xi=kx^{\frac{1-m}{2}}$ (Kafoussias and Nanousis [19]) is the dimensionless distance along the wedge ($\xi>0$).

The system of Eqs. (17) to (19) can also be written as

$$f'''+\frac{(\theta-\theta_r)}{\theta_r}\left\{ff''+\frac{2}{1+m}\gamma_1(\theta+N\phi)\sin\frac{\Omega}{2}-\frac{2}{m+1}\xi^2\lambda(f'-1)-\frac{2}{m+1}(f'^2-1)\left(\frac{\mathrm{Re}\,x}{\mathrm{Re}_k}F_n+m\right)\right.$$
$$\left.-\lambda_u(2-2f'-\eta f'')\right\}-\frac{2}{1+m}\left(\frac{1}{\theta-\theta_r}\right)\theta' f''=-\frac{(\theta-\theta_r)}{\theta_r}\frac{1-m}{1+m}\xi\left(f''\frac{\partial f}{\partial \xi}-f'\frac{\partial f'}{\partial \xi}\right) \tag{21}$$

$$\theta''+\mathrm{Pr}_A\,f\theta'-\frac{2\mathrm{Pr}_A}{1+m}f'\theta+\mathrm{Pr}_A\,E_c f''^2+\mathrm{Pr}_A\,\lambda_u\eta\theta'=-\mathrm{Pr}_A\frac{1-m}{1+m}\xi\left(\theta'\frac{\partial f}{\partial \xi}-f'\frac{\partial \theta}{\partial \xi}\right) \tag{22}$$

$$\phi''+Sc(f-\tau\theta')\phi'-\frac{2Sc}{1+m}\phi f'-Sc\tau\theta''\phi-\frac{2Sc}{1+m}\xi^2\gamma\phi+Sc\lambda_u\eta\phi'=-Sc\frac{1-m}{1+m}\xi\left(\phi'\frac{\partial f}{\partial \xi}-f'\frac{\partial \phi}{\partial \xi}\right) \tag{23}$$

with boundary conditions

$$f'(\xi,0)=0,\qquad \frac{(1+m)}{2}f(\xi,0)+\frac{1-m}{2}\xi\frac{\partial f(\xi,0)}{\partial \xi}=-S,\qquad \theta(\xi,0)=1,\qquad \phi(\xi,0)=1$$
$$f'(\xi,\infty)=1,\qquad \theta(\xi,\infty)=0,\qquad \phi(\xi,\infty)=0 \tag{24}$$

It may be observed that Eqs. (21)–(23) with boundary conditions (24) remain partial differential equations after transformation, with $\frac{\partial}{\partial \xi}$ terms on the right-hand side. In this system of equations, it is obvious that the nonsimilarity aspects of the problem are embodied in the terms containing partial derivatives with respect to n. This problem does not admit similarity solutions. Thus, with ξ-derivative terms retained in the system of equations, it is necessary to employ a numerical scheme suitable for partial differ-

ential equations for the solution. Formulation of the system of equations for the local nonsimilarity model with reference to the present problem will now be discussed.

At the first level of truncation, the terms accompanied by $\xi\frac{\partial}{\partial\xi}$ are small. This is particularly true when $\xi \ll 1$. Thus the terms with $\xi\frac{\partial}{\partial\xi}$ on the right-hand sides of Eqs. (21)–(23) are deleted to get the following system of equations:

$$\begin{aligned} &f''' + \frac{(\theta-\theta_r)}{\theta_r}\left\{ ff'' + \frac{2}{1+m}\gamma_1(\theta+N\phi)\sin\frac{\Omega}{2} \right. \\ &\quad - \frac{2}{m+1}\xi^2\lambda(f'-1) \\ &\quad - \frac{2}{m+1}(f'^2-1)\left(\frac{\mathrm{Re}\,x}{\mathrm{Re}_k}F_n + m\right) \\ &\quad \left. - \lambda_u(2-2f'-\eta f'')\right\} - \frac{2}{1+m}\left(\frac{1}{\theta-\theta_r}\right)\theta' f'' \\ &= 0 \end{aligned} \tag{25}$$

$$\theta'' + \mathrm{Pr}_A\, f\theta' - \frac{2\,\mathrm{Pr}_A}{1+m}f'\theta + \mathrm{Pr}_A\, E_c f''^2 + \mathrm{Pr}_A\,\lambda_u\eta\theta' = 0 \tag{26}$$

$$\begin{aligned} &\phi'' + Sc(f-\tau\theta')\phi' - \frac{2Sc}{1+m}\phi f' - Sc\tau\theta''\phi \\ &\quad - \frac{2Sc}{1+m}\xi^2\gamma\phi + Sc\lambda_u\eta\phi' = 0 \end{aligned} \tag{27}$$

with boundary conditions

$$\begin{aligned} &f'(0)=0, \qquad \frac{(1+m)}{2}f(0) = -S, \\ &\theta(0)=1, \qquad \phi(0)=1 \\ &f'(\infty)=1, \qquad \theta(\infty)=0, \qquad \phi(\infty)=0 \end{aligned} \tag{28}$$

From the definition of Prandtl number, we see that it is a function of viscosity, and as the viscosity varies across the boundary layer, the Prandtl number also varies. The assumption of constant Prandtl number inside the boundary layer may produce unrealistic results [21–24]. Therefore, the Prandtl number related to the variable viscosity is defined as

$$\mathrm{Pr}_v = \frac{\mu_v c_p}{k_e} = \frac{\mu[\frac{\theta_r}{\theta_r-\theta}]c_p}{k_e} = \left[\frac{\theta_r}{\theta_r-\theta}\right]\mathrm{Pr}_A \tag{29}$$

At the surface ($\eta = 0$) of the wedge, it can be defined as $\mathrm{Pr}_v = [\frac{\theta_r}{\theta_r-\theta}]\mathrm{Pr}_A$.

From Eq. (29), it can be seen that for $\theta_r \to \infty$, the variable Prandtl number Pr_v is equal to the ambient Prandtl number Pr_A. For $\eta \to \infty$, i.e. outside the boundary layer, $\theta(\eta)$ becomes zero; therefore, Pr_v equals Pr_A regardless of the values of θ_r.

Equation (26) can be expressed as

$$\begin{aligned} &\theta'' + \left(1-\frac{\theta}{\theta_r}\right)\mathrm{Pr}_v\, f\theta' - \frac{2}{1+m}\left(1-\frac{\theta}{\theta_r}\right)\mathrm{Pr}_v\, f'\theta \\ &\quad + \left(1-\frac{\theta}{\theta_r}\right)\mathrm{Pr}_v\, E_c f''^2 + \left(1-\frac{\theta}{\theta_r}\right)\mathrm{Pr}_v\,\lambda_u\eta\theta' \\ &= 0 \end{aligned} \tag{30}$$

Further, we suppose that $\lambda_u = \frac{c}{x^{m-1}}$ where c is a constant so that $c = \frac{\delta^m}{\nu}\frac{d\delta}{dt}$ and integrating, it is obtained that

$$\delta = \left[c(m+1)\nu t\right]^{\frac{1}{m+1}} \tag{31}$$

When $c = 2$ and $m = 1$ in Eq. (31) and we get $\delta = 2\sqrt{\nu t}$ which shows that the parameter δ can be compared with the well established scaling parameter for the unsteady boundary layer problems (see Schlichting [25]).

The major physical quantities of interest are the local skin friction coefficient; the local Nusselt number and the local Sherwood number are defined, respectively, by:

$$\begin{aligned} &C_f = \frac{f''(0)}{\mathrm{Re}_x^{\frac{1}{2}}}; \qquad N_u = -\frac{\theta'(0)}{\mathrm{Re}_x^{\frac{1}{2}}} \quad \text{and} \\ &S_h = -\frac{\phi'(0)}{\mathrm{Re}_x^{\frac{1}{2}}} \end{aligned} \tag{32}$$

The momentum equation (25) can also be attempt these circumstances if one takes $\gamma_1 \gg 1.0$ corresponds to pure free convection, $\gamma_1 = 1.0$ corresponds to mixed convection and $\gamma_1 \ll 1.0$ corresponds to pure forced convection. γ is the chemical reaction parameter in Eq. (27) can be adjusted to meet these circumstances if one takes (i) $\gamma > 0$ for destructive reaction, (ii) $\gamma = 0$ for no reaction and (iii) $\gamma < 0$ for generative reaction. Throughout this calculation we have considered $\gamma_1 = 1.0$ unless otherwise specified. This form of the system is the most suitable for the application of the numerical scheme described below.

3 Numerical solution

The unsteady boundary layer over the wedge, subjected to the velocity of suction or injection, is described by the system of ordinary differential equations (25), (27), (30) and its boundary conditions (28). A modified and improved numerical solution scheme, for local nonsimilarity boundary layer analysis, is

Table 1 Comparison of the current results with previous published work for $\beta_1 = \lambda_u = 0$

η	White [29]			Present works		
	$f(\eta)$	$f'(\eta)$	$f''(\eta)$	$f(\eta)$	$f'(\eta)$	$f''(\eta)$
0.0	0.00000	0.000000	0.469599	0.000000	0.000000	0.469686
0.5	0.05864	0.23423	0.46503	0.058656	0.234267	0.465078
1.0	0.23299	0.46063	0.43438	0.232986	0.460628	0.434377
2.0	0.88680	0.81669	0.25567	0.886797	0.816687	0.255668
3.0	1.79557	0.96905	0.06771	1.795569	0.969046	0.067714
4.0	2.78388	0.99777	0.00687	2.783882	0.997773	0.006871
5.0	3.78323	0.99994	0.00026	3.783234	0.999941	0.000262

used. The scheme is similar to that of Minkowycz and Sparrow [26] but it deals with the differential equations in lieu of integral equations. In each level of truncation, the governing coupled and nonlinear system of differential equations is solved by applying the common finite difference method, with central differencing, a tridiagonal matrix manipulation, and an iterative procedure. The whole numerical scheme can be programmed and applied easily and has distinct advantages compared to that in Minkowycz and Sparrow [26] with respect to stability, accuracy, and convergence speed. The details of this scheme are described in Kafoussias and Karabis [27] and Kafoussias and Williams [28].

To examine the behavior of the unsteady boundary layer over the wedge, numerical calculations were carried out for different values of the dimensionless parameters, entering the problem under consideration for $\mathrm{Pr}_v = 1.42$, which corresponds to air. The numerical results are shown in Figs. 2–12 for the velocity, the temperature and the concentration of the fluid along the wall of wedge.

4 Results and discussion

For the purpose of discussing the effects of various parameters on the flow behavior near the wedge surface, numerical calculations have been carried out for different values of τ, λ, λ_u, Pr_v, Sc, N, γ, θ_r and γ_1. When viscosity does not depend on the temperature, then the values of the Prandtl number $\mathrm{Pr}_A = 0.71$, 2.97 and 7.0 correspond to air, Methyl chloride and water. As viscosity depends on the temperature, then these values at the surface of the wedge ($\eta = 0$) and for $\theta_r = 2.0$ ($\eta = 0$) correspond to $\mathrm{Pr}_v = 1.42$, 5.94 and 14. The values of Schmidt number Sc are taken for hydrogen ($Sc = 0.22$), helium ($Sc = 0.30$), water-vapour ($Sc = 0.62$) and carbon-dioxide ($Sc = 0.94$). It is also worth mentioning that according to the definition of the thermophoresis parameter, $\tau > 0$. A positive value of τ implies the lower surface temperature T_w compared to the ambient temperature of the fluid T_∞, i.e. $T_w < T_\infty$. A positive value of τ further implies that $E_c < 0$. The velocity, temperature and concentration profiles obtained in the dimensionless form are presented in the following figures for $\mathrm{Pr}_v = 1.42$, $\beta_1 = \frac{1}{3}(\Omega = 60^0)$, $Sc = 0.62$, $Nt = 2.0$ and $\theta_r = 2.0$, $\lambda = 0.1$, $E_c = -0.001$, Grashof number for heat transfer is chosen to be $Gr_x = 9$, since these values (Gr_x) corresponds to a cooling problem and Reynolds number $\mathrm{Re}_x = 3.0$, unless otherwise stated.

Numerical computations have been carried out for various values of unsteady parameter (λ_u), variable viscosity θ_r, thermophoresis particle deposition parameter (τ) and chemical reaction parameter (γ). In order to validate our method, we have compared the results of $f(\eta)$, $f'(\eta)$ and $f''(\eta)$ for various values of η (Table 1) with those of White [29] and found them in excellent agreement.

In the absence of diffusion equation with steady flow, in order to ascertain the accuracy of our numerical results, the present study is compared with the available exact solution in the literature. The velocity profiles for ξ are compared with the available exact solution of Minkowycz and Sparrow [26], is shown in Fig. 2. It is observed that the agreements with the theoretical solution of velocity and temperature profiles are excellent.

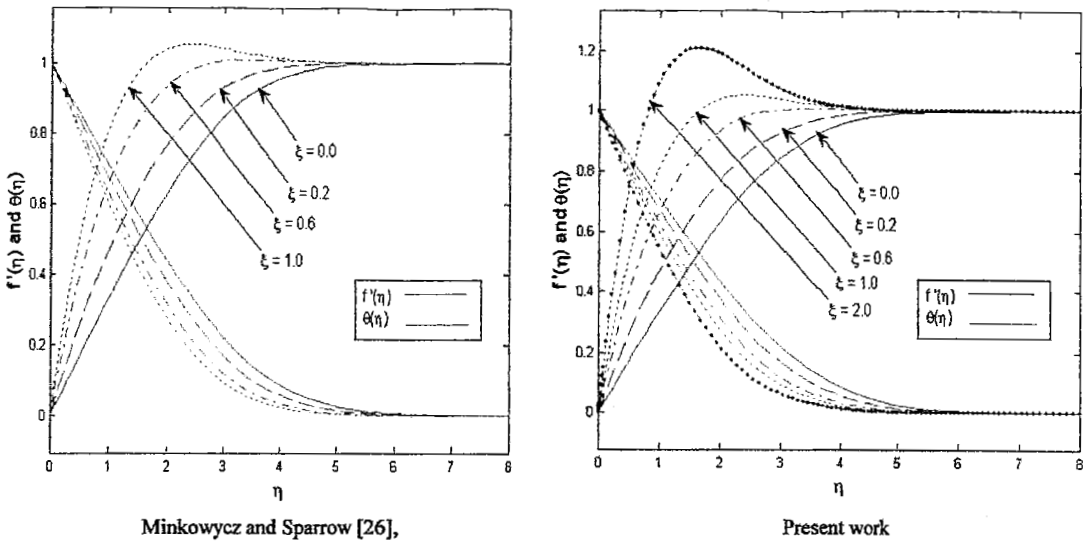

Fig. 2 Comparison of the velocity profiles with Minkowycz and Sparrow [26]

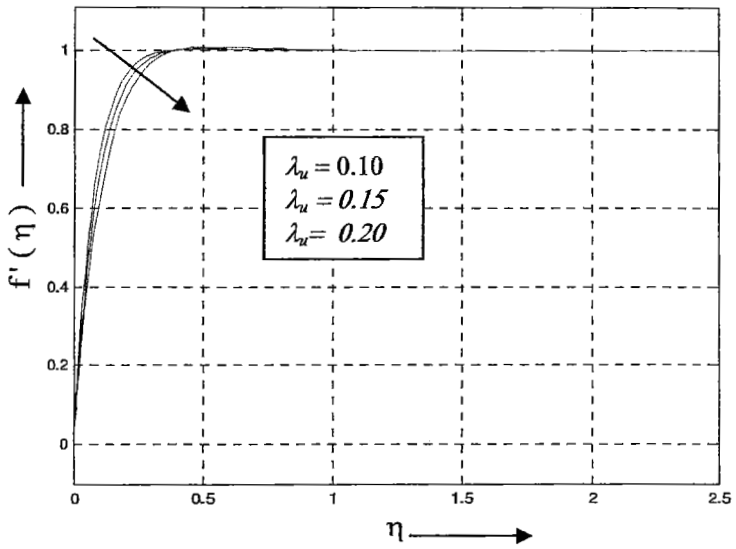

Fig. 3 Unsteadiness effect on velocity profiles. $\gamma_1 = 1.0$, $m = 0.0909$, $\gamma = \mathrm{Re}_k = 1.0$, $N = 3$, $\tau = 0.5$, $F_n = 0.1$, $S = 3.0$, $\xi = 0.01$ and $\Omega = 30^0$

The effects of unsteadiness parameter λ_u on the dimensionless velocity, temperature and concentration profiles within the boundary-layer have been displayed in Figs. 3, 4 and 5, respectively. From these figures, it is observed that the velocity profile decreases whereas the temperature and concentration profiles increase with the increase of unsteadiness parameter λ_u. The variation of the Prandtl number within the boundary layer for different values of the unsteadiness parameter λ_u play a very important role on flow field and it is clearly observed that an increase in λ_u decreases Pr_v within the boundary layer. The reason for this behavior is that the inertia of the porous medium provides an additional resistance to the fluid flow mechanism, which causes the fluid to move at a retarded rate with reduced velocity.

Effect of thermophoresis parameter τ on concentration field is shown in Fig. 6. It is observed that the concentration of the fluid decreases with increase of thermophoretic parameter whereas the velocity and temperature of the fluid are not significant with increase

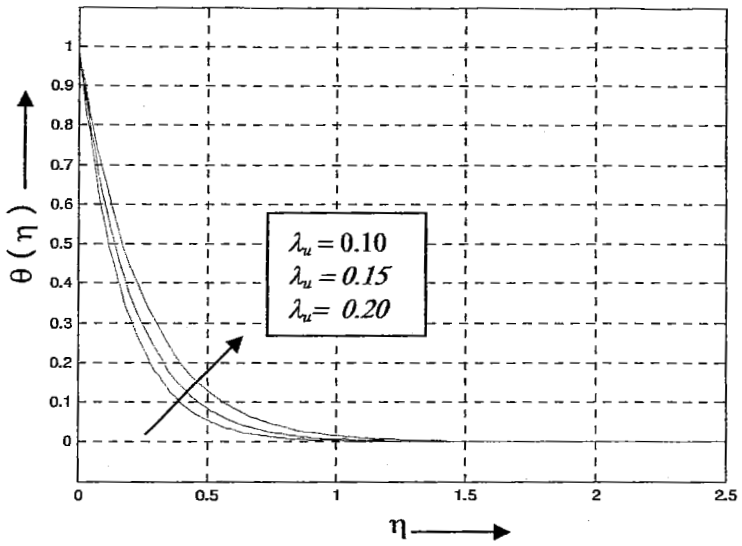

Fig. 4 Unsteadiness effect on temperature profiles. $\gamma_1 = 1.0$, $m = 0.0909$, $\gamma = \mathrm{Re}_k = 1.0$, $N = 3$, $\tau = 0.5$, $F_n, \lambda = 0.1$, $S = 3.0$, $\theta_r = 2.0$, $\xi = 0.01$ and $\Omega = 30^0$

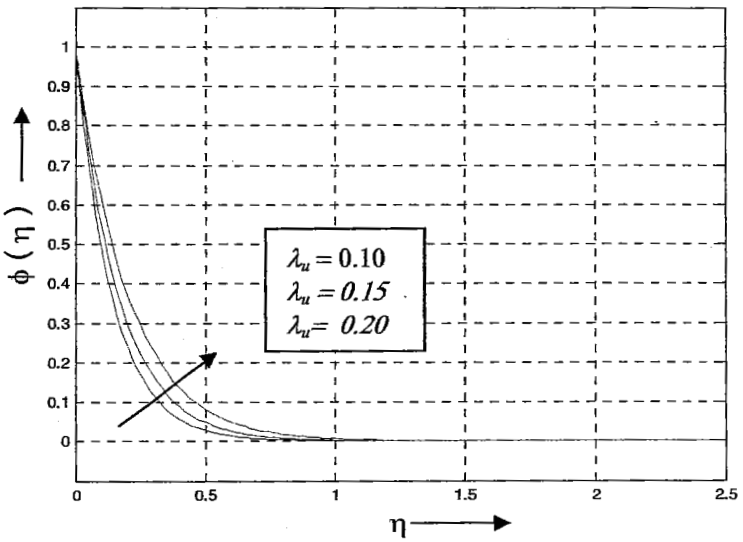

Fig. 5 Unsteadiness effect on concentration profiles. $\gamma_1 = 1.0$, $m = 0.0909$, $\gamma = \mathrm{Re}_k = 1.0$, $\tau = 0.5$, $N = 3$, $F_n = 0.1$, $S = 3.0$, $\xi = 0.01$ and $\Omega = 30^0$

of thermophoretic parameter. In particular, the effect of increasing the thermophoretic parameter τ is limited to increasing slightly the wall slope of the concentration profiles but decreasing the concentration. This is true only for small values of Schmidt number for which the Brownian diffusion effect is large compared to the convection effect. However, for large values of Schmidt number, the diffusion effect is minimal compared to the convection effect and, therefore, the thermophoretic parameter τ is expected to alter the concentration boundary layer significantly. This is consistent with the work of Alam et al. [5] on thermophoresis of aerosol particles in flat plate boundary layer. The effect of viscosity on velocity and temperature profiles is shown in Figs. 7 and 8 respectively. It is seen that the velocity of the fluid increases with increase of viscosity while the thermal boundary layer thickness decreases as the viscosity increases. So, the increase of viscosity accelerates the fluid motion and reduces the temperature of the fluid along the wall. This

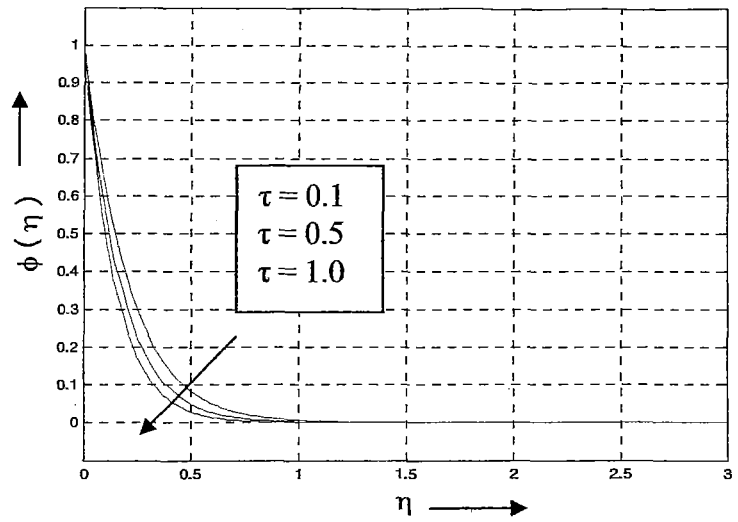

Fig. 6 Thermophoretic effect on concentration profiles. $\gamma_1 = 1.0$, $m = 0.0909$, $\gamma = \mathrm{Re}_k = 1.0$, $N = 3$, $F_n, \lambda = 0.1$, $S = 3.0$, $\lambda_u = 0.1$ and $\Omega = 30^0$

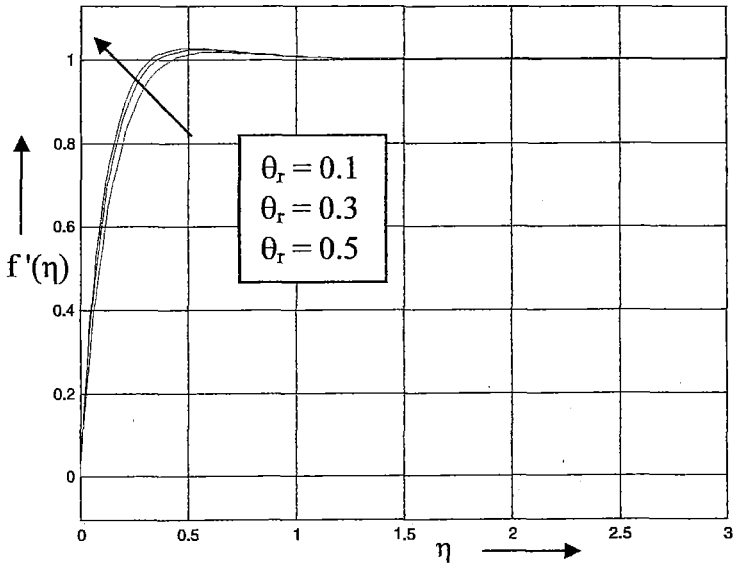

Fig. 7 Viscosity effect on velocity profiles. $\gamma_1 = 1.0$, $m = 0.0909$, $\mathrm{Re}_k = 1.0$, $N = 3$, $F_n = \lambda_u = 0.1$, $S = 3.0$, $\tau = 0.5$, $\xi = 0.01$ and $\Omega = 30^0$

figure also confirmed us that when θ_r becomes very large, variations in the temperature profiles become less pronounced, since Eq. (30) implies that $\mu \to \mu_\infty$ as $\theta_r \to \infty$. Also, it is observed that the concentration of the fluid is almost not affected with increase of the viscosity.

Figures 9, 10 and 11 represents the dimensionless velocity, temperature and concentration profiles for different values of buoyancy parameter. In the presence of uniform porosity effect, it is clear that the velocity for free convection is more dominant compared to the forced and mixed convection flow whereas the temperature and the concentration of the fluid for forced convection is monotonically dominant compared to the other buoyancy forces.

Figure 12 represents the dimensionless concentration profiles $\phi(\eta)$ for different values of the chemical reaction parameter. For uniform suction and temperature-dependent fluid viscosity, an increase in chemical reaction, leads to fall in concentration of the

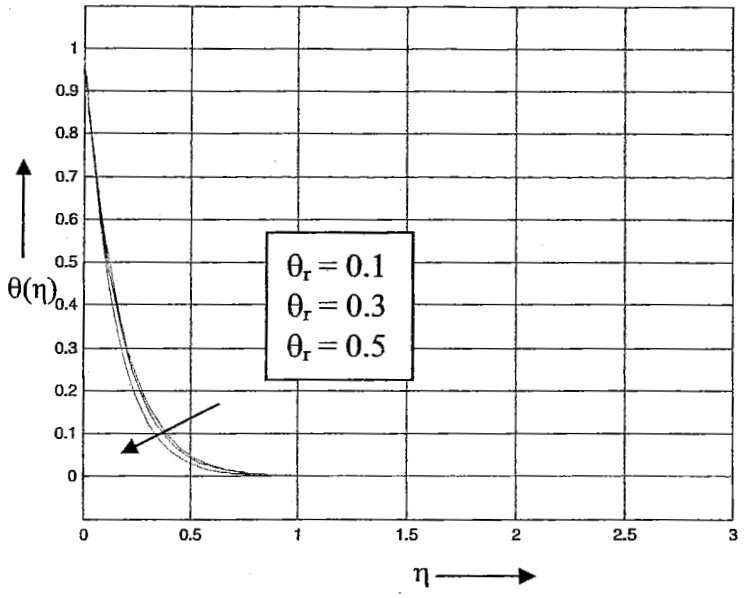

Fig. 8 Viscosity effect on temperature profiles. $\gamma_1 = 1.0$, $m = 0.0909$, $\mathrm{Re}_k = 1.0$, $N = 3$, F_n, $\lambda_u = 0.1$, $S = 3.0$, $\tau = 0.5$, $\xi = 0.01$ and $\Omega = 30^0$

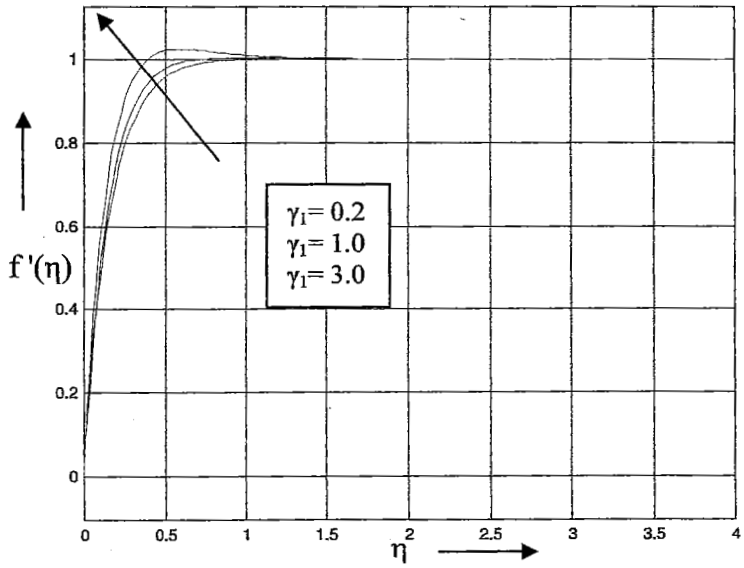

Fig. 9 Buoyancy effects on velocity profiles. $\gamma = 1.0$, $m = 0.0909$, $\mathrm{Re}_k = 1.0$, $N = 3$, $\lambda_u = 0.1$, $S = 3.0$, $\tau = 0.5$, $\xi = 0.01$ and $\Omega = 30^0$

fluid along the wall of the surface and these are shown in Fig. 12. So, in the case of suction, the chemical reaction decelerates the concentration of the fluid along the wall of the surface whereas the velocity and the temperature of the fluid are not significant with increase of chemical reaction parameter. It is observed that the effects of destructive reaction on the concentration profiles are much more pronounced than that of the generative reaction. In particular, the concentration of the fluid gradually changes from higher value to the lower value only when the strength of rate of chemical reaction k_1 is higher than the kinematic viscosity ν of the fluid.

From Table 2, it is observed that the skin friction increases and the rate of heat and mass transfer decrease with increase of chemical reaction and un-

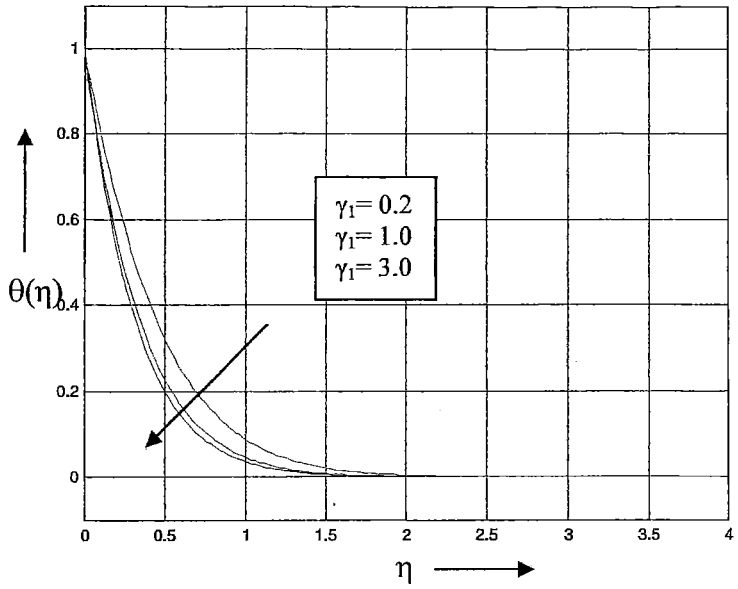

Fig. 10 Buoyancy effects on temperature profiles. $m = 0.0909$, $\mathrm{Re}_k = 1.0$, $N = 3$, $\lambda = 0.1$, $E_c = 0.001$, $S = 3.0$, $\tau = 0.5$, $\xi = 0.01$ and $\Omega = 30^0$

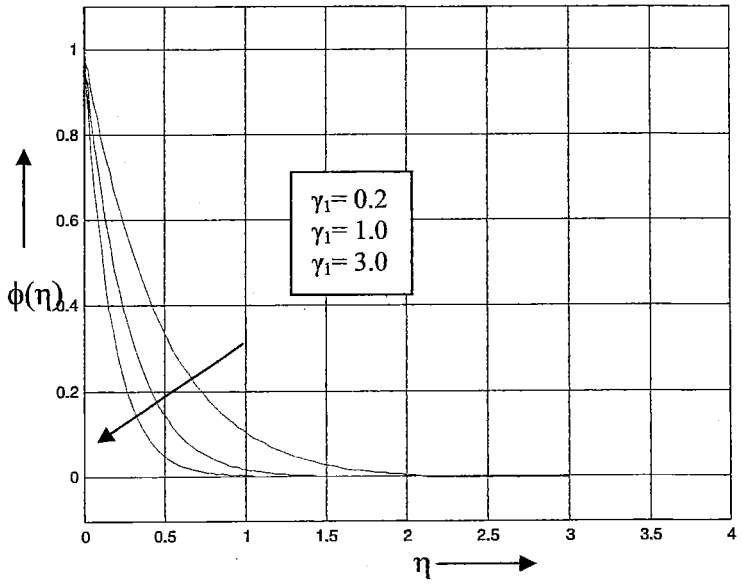

Fig. 11 Buoyancy effects on concentration profiles. $\gamma = 1.0$, $m = 0.0909$, $\mathrm{Re}_k = 1.0$, $N = 3$, $\lambda_u = 0.1$, $S = 3.0$, $\tau = 0.5$, $\xi = 0.01$ and $\Omega = 30^0$

steadiness parameters respectively, whereas the skin friction and the rate of mass transfer decrease and the rate of heat transfer increases with increase of thermophoretic parameters. It is interesting to note that the rate of change of skin friction and mass transfer of forced convection flow are more significant to compare with free and mixed convection flows whereas the rate of change of heat transfer of free convection flow is faster than the other two buoyancy forces. The variation of the Prandtl number within the boundary layer for different values of the unsteadiness parameter λ_u is plotted in Table 3. It is noticed that an increase in λ_u decreases Pr_v within the boundary layer.

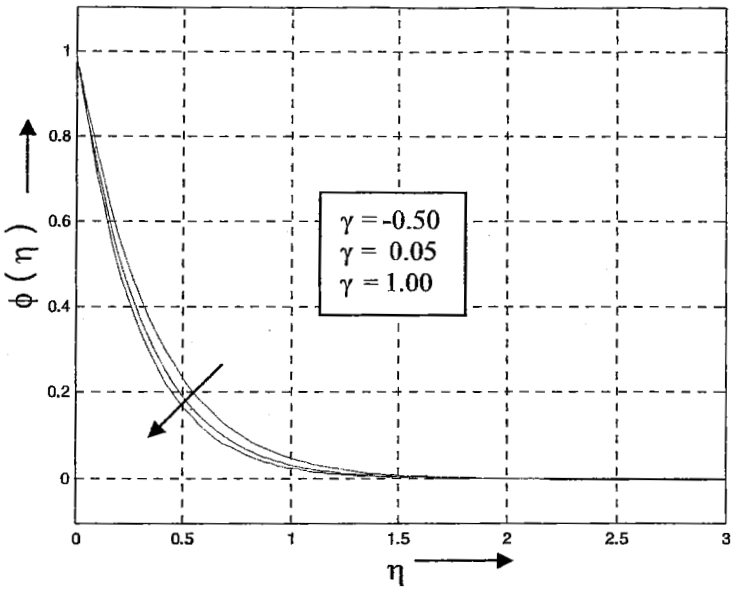

Fig. 12 Chemical reaction effects on concentration profiles. $\gamma_1 = 1.0$, $m = 0.0909$, $\mathrm{Re}_k = 1.0$, $N = 3$, $\lambda_u = 0.1$, $S = 3.0$, $\tau = 0.5$, $\xi = 0.01$ and $\Omega = 30^0$

Table 2 Analysis for skin friction and rate of heat and mass transfer

$f''(0)$	$\theta'(0)$	$\phi'(0)$	Parameter	
0.734312	−1.162571	−1.423467	$\tau = 1.0$	Thermophoretic parameter
0.734211	−1.162522	−1.724122	$\tau = 2.0$	
0.734052	−1.162497	−1.976543	$\tau = 3.0$	
1.123717	−1.238325	−1.123741	$\gamma = 0.1$	Chemical reaction parameter
1.123734	−1.238359	−1.123972	$\gamma = 1.5$	
1.123749	−1.238387	−1.124032	$\gamma = 2.5$	
1.119227	−1.314271	−1.213467	$\lambda_u = 0.05$	Unsteadiness parameter
1.434241	−1.456174	−1.282889	$\lambda_u = 0.10$	
1.673272	−1.498684	−1.588722	$\lambda_u = 0.30$	
1.084562	−1.156182	−1.732578	$\gamma_1 = 0.1$	Forced convection parameter
1.185181	−1.157219	−1.747165	$\gamma_1 = 1.0$	Mixed convection parameter
1.238161	−1.159184	−1.783641	$\gamma_1 = 5.0$	Free convection parameter

5 Conclusions

In the present paper, the effect of variable viscosity on unsteady non-Darcy mixed convection boundary layer flow over a porous wedge with thermophoresis particle deposition in the presence of chemical reaction has been studied numerically. There are many parameters involved in the final form of the mathematical model. The problem can be extended on many directions, but the first one seems to be to consider the effects of chemical reaction with thermophoresis particle deposition.

- In the presence of uniform viscosity, it is interesting to note that the velocity of the fluid decreases with increase of unsteadiness parameter. In unsteady mixed convective non-Darcy flow regime, the concentration boundary layer thickness decreases with increase of the thermophoretic and chemical reaction parameters.

Table 3 Analysis of Pr_v for different values of unsteadiness parameter, λ_u

η	Pr_v		
	$\lambda_u = 0.0$	$\lambda_u = 0.05$	$\lambda_u = 0.10$
0.0	1.439620	1.426867	1.404417
1.0	1.289026	1.275599	1.252721
2.0	1.153822	1.143275	1.125874
3.0	0.801371	0.740450	0.723370
4.0	0.712785	0.708037	0.706851

- Destructive reaction plays a dominant role on concentration field compared to generative reaction.
- In the presence of uniform porosity, it is clear that the velocity for free convection is more dominant compared to the forced and mixed convection flow whereas the temperature and the concentration of the fluid for forced convection is monotonically dominant compared to the other buoyancy forces.
- It is interesting to note that the thermophoretic with chemical reaction effects in the presence of unsteady flow field have a substantial effect on the flow field and, thus, on the heat and mass transfer rate from the sheet to the fluid.
- Thermophoresis is an important mechanism of micro-particle transport due to a temperature gradient in the surrounding medium and has found numerous applications, especially in the field of aerosol technology.

It is interesting to note that the chemical reaction effect in the presence of thermophoresis particle deposition on dust particle play a very important role on Global warming. Acid gas reactions during the passage from the source regions to the western North Pacific modify the chemical characteristics of Asian mineral dust particles as they pass through heavily industrial regions. The high adsorption of HNO_3 on mineral dust particles would change their surface properties from hydrophobic to hygroscopic and form an efficient mechanism to remove nitrogen compounds to the ocean surface layer. In addition, dust particles make important contributions to regional and/or global climate and environment changes because particle can scatter and/or absorb solar radiation, act as chemical reaction sites in the atmosphere. Since oxidation has a strong effect on particle lifetime in the atmosphere, these results will help climate scientists refine the computer models used to predict climate change.

Acknowledgements The authors wish to express their cordial thanks to our beloved The Vice Chancellor and The Dean, Faculty of Science, technology and Human Development, Universiti Tun Hussein Onn Malaysia, for their encouragements.

References

1. Tsai R, Lin ZY (1999) An approach for evaluating aerosol particle deposition from a natural convection flow onto a vertical flat plate. Journal of Hazardous Materials 69:217–227
2. Selim A, Hossain MA, Rees DAS (2003) The effect of surface mass transfer on mixed convection flow past a heated vertical flat permeable plate with thermophoresis. Int J Therm Sci 42:973–982
3. Seddeek MA (2006) Influence of viscous dissipation and thermophoresis on Darcy-Forchheimer mixed convection in a fluid saturated porous media. J Colloid Interface Sci 293:137–142
4. Postelnicu A (2007) Effects of thermophoresis particle deposition in free convection boundary layer from a horizontal flat plate embedded in a porous medium. Int J Heat Mass Transf 50:2981–2985
5. Alam MS, Rahman MM, Sattar MA (2008) Effects of variable suction and thermophoresis on steady MHD combined free-forced convective heat and mass transfer flow over a semi-infinite permeable inclined flat plate in the presence of thermal radiation. Int J Therm Sci 47:758–765
6. Alam MS, Rahman MM, Sattar MA (2008) Effects of chemical reaction and thermophoresis on MHD mixed convective heat and mass transfer flow along an inclined plate in the presence of heat generation/absorption with viscous dissipation and joule heating. Can J Phys 86:1057–1066
7. Alam MS, Rahman MM, Sattar MA (2009) On the effectiveness of viscous dissipation and Joule heating on steady magnetohydrodynamic heat and mass transfer flow over an inclined radiate isothermal permeable surface in the presence of thermophoresis. Commun Nonlinear Sci Numer Simul 4:2132–2143
8. Goldsmith P, May FG (1966) Diffusiophoresis and thermophoresis in water vapour systems. In: Davies CN (ed) Aerosol science. Academic Press, London, pp 163–194
9. Goren SL (1977) Thermophoresis of aerosol particles in laminar boundary layer on flat plate. J Colloid Interface Sci 61:77–85
10. Jayaraj S, Dinesh KK, Pallai KL (1999) Thermophoresis in natural convection with variable properties. Heat Mass Transf 34:469–475
11. Hales JM, Schwendiman LC, Horst TW (1972) Aerosol transport in a naturally-convected boundary layer. Int J Heat Mass Transf 15:1837–1849
12. Chamkha JA, Al-Mudhaf FA, Pop I (2006) Effects of heat generation or absorption on thermophoretic free convection boundary layer from a vertical flat plate embedded in a porous medium. Int Commun Heat Mass Transf 33:1096–1102
13. Chamkha JA, Pop I (2004) Effects of thermophoresis particle deposition in free convection boundary layer from a vertical flat plate embedded in a porous medium. Int Commun Heat Mass Transf 31:421–430

14. Duwairi HM, Damseh RA (2008) Effect of thermophoresis particle deposition on mixed convection from vertical surface embedded in saturated porous medium. Int J Numer Methods Heat Fluid Flow 18:202–216
15. Rahman MM, Postelnicu A (2010) Effects of thermophoresis on the forced convective laminar flow of a viscous incompressible fluid over a rotating disk. Mech Res Commun 37:598–603
16. Sattar MA (2011) A local similarity transformation for the unsteady two-dimensional hydrodynamic boundary layer equations of a flow past a wedge. Int J Appl Math Mech 7:15–28
17. Talbot L, Cheng RK, Schefer AW, Wills DR (1980) Thermophoresis of particles in a 552 heated boundary layer. J Fluid Mech 101:737–758
18. Pantokratoras A (2006) The Falkner-Skan flow with constant wall temperature and variable viscosity. Int J Therm Sci 45:378–385
19. Kafoussias NG, Nanousis ND (1997) Magnetohydrodynamic laminar boundary layer flows over a wedge with suction or injection. Can J Phys 75:733–741
20. Sattar MA (1994) Unsteady hydromagnetic free convection flow with Hall current, mass transfer and variable suction through a porous medium near an infinite vertical porous plate with constant heat flux. Int J Energy Res 18:771–775
21. Pantokratoras A (2005) Forced and mixed convection boundary layer flow along a flat plate with variable viscosity and variable Prandtl number, new results. Heat Mass Transf 41:1085–1094
22. Pantokratoras A (2007) Non-Darcian forced convection heat transfer over a flat plate in a porous medium with variable viscosity and variable Prandtl number. J Porous Media 10:201–208
23. Rahman MM, Rahman MA, Samad MA, Alam MS (2009) Heat transfer in micropolar fluid along a non-linear stretching sheet with temperature dependent viscosity and variable wall temperature. Int J Thermophys 30:1649–1670
24. Rahman MM, Salauddin KM (2010) Study of hydromagnetic heat and mass transfer flow over an inclined heated surface with variable viscosity and electric conductivity. Commun Nonlinear Sci Numer Simul 15:2073–2085
25. Schlichting H (1968) Boundary layer theory. McGraw Hill, New York
26. Minkowycz WJ, Sparrow EM, Schneider GE, Pletcher RH (1988) Handbook of numerical heat transfer. Wiley, New York, pp 192–195
27. Kafoussias NG, Karabis AG (1996) In: Sotiropoulos DA, Greek DEB (eds) Proceedings of the 2nd national congress on computational mechanics, Chania, Greece, June 26–28, 1996, vol II. Greek Association of Computational Mechanics, Member of IACM, pp 801–809
28. Kafoussias NG, Williams EW (1993) Improved approximation technique to obtain numerical solution of a class of two-point boundary value similarity problems in fluid mechanics. Int J Numer Methods Fluids 17:145–152
29. White FM (2006) Viscous fluid flows, 3rd edn. McGraw-Hill, New York